Computer Modeling in Engineering & Sciences

Tech Science Press

Doi:10.32604/cmes.2025.067702

ARTICLE

Explicit ARL Computational for a Modified EWMA Control Chart in Autocorrelated Statistical Process Control Models

Yadpirun Supharakonsakun[1], **Yupaporn Areepong**[2] **and Korakoch Silpakob**[3,*]

[1]Department of Applied Mathematics and Statistics, Phetchabun Rajabhat University, Phetchabun, 67000, Thailand
[2]Department of Applied Statistics, King Mongkut's University of Technology North Bangkok, Bangkok, 10800, Thailand
[3]Department of Educational Testing and Research, Buriram Rajabhat University, Buriram, 31000, Thailand

*Corresponding Author: Korakoch Silpakob. Email: korakoch.sk@bru.ac.th

Received: 09 May 2025; Accepted: 28 September 2025; Published: 30 October 2025

ABSTRACT: This study presents an innovative development of the exponentially weighted moving average (EWMA) control chart, explicitly adapted for the examination of time series data distinguished by seasonal autoregressive moving average behavior—SARMA$(1,1)_L$ under exponential white noise. Unlike previous works that rely on simplified models such as AR(1) or assume independence, this research derives for the first time an exact two-sided Average Run Length (ARL) formula for the Modified EWMA chart under SARMA$(1,1)_L$ conditions, using a mathematically rigorous Fredholm integral approach. The derived formulas are validated against numerical integral equation (NIE) solutions, showing strong agreement and significantly reduced computational burden. Additionally, a performance comparison index (PCI) is introduced to assess the chart's detection capability. Results demonstrate that the proposed method exhibits superior sensitivity to mean shifts in autocorrelated environments, outperforming existing approaches. The findings offer a new, efficient framework for real-time quality control in complex seasonal processes, with potential applications in environmental monitoring and intelligent manufacturing systems.

KEYWORDS: Statistical process control; average run length; modified EWMA control chart; autocorrelated data; SARMA process; computational modeling; real-time monitoring

1 Introduction

To guarantee that products and services achieve certain standards, particularly in manufacturing and service industries, quality control is vital. Effective monitoring and control processes are essential for maintaining product consistency and meeting customer expectations. Statistical process control (SPC) provides a robust framework for refining process quality through various analytical tools, of which control charts are an important tool. Many businesses make extensive use of these charts to track procedure performance and ascertain shifts in procedure averages, which are crucial markers of process consistency [1–4]. Initially presented by Shewhart [5], conventional control charts remain the basic tool for identifying large and significant changes in a process. However, their effectiveness is reduced when smaller, more subtle deviations are detected, which are often important for the early detection of process problems. Researchers have developed alternative control charts tailored to pinpoint substantial and minor changes to address the limitations of Shewhart charts. Among these innovations, the Cumulative Sum Control Chart (CUSUM) described by Page [6] has been acknowledged for its exceptional ability to distinguish minor alterations in the process mean compared to the Shewhart chart [7–9]. Similarly, Roberts [10] introduced the Exponential

Copyright © 2025 The Authors. Published by Tech Science Press.
This work is licensed under a Creative Commons Attribution 4.0 International License, which permits unrestricted use, distribution, and reproduction in any medium, provided the original work is properly cited.

Weighted Moving Average (EWMA) control chart, which has demonstrated its efficiency in perceiving minor changes, especially when dealing with non-independent or non-normally distributed data [11–13]. The EWMA chart offers a more responsive detection mechanism for small changes, complementing existing tools in SPC. Based on the EWMA framework, Khan et al. [14] presented a modified EWMA statistic, integrating supplementary constants to describe past and present process behavior [15]. This modification is particularly useful when the data shows deviations from the assumptions of independence or normality, which are common in many real-world processes [16–19].

Particularly when assessed with the average running length (ARL) in mind, a significant aspect of control chart execution, spotlighting recent data makes the modified EWMA chart outpace long-established approaches [20–22]. The ARL shows the typical number of events that must happen in order for the control chart to alert us that this particular operation is no longer under control. Moreover, it is divided into two main components, ARL_0 and ARL_1. ARL_0 represents the mean time that the process can be considered in control, which should ideally be maximized, while ARL_1 measures the rapidity with which the control chart can distinguish processes that are not in control, and ought to be minimized. Many different methodologies have been used to estimate the ARL, comprising Monte Carlo simulations, Markov chain approaches, and numerical integral equations (NIE). Of these, explicit formulas derived from the integral equations have been proven to be particularly effective for estimating the ARL. For example, Crowder [23] used an integral equation procedure for ARL assessment for Gaussian processes on EWMA control charts, while Champ and Rigdon [24] used a similar approach with CUSUM and EWMA charts, comparing the outcomes gained with Markov Chain simulations. Fredholm's integral equation has also been widely used to estimate the ARL, demonstrating its effectiveness in various control chart setups [25–27]. Despite these advances, standard EWMA charts can sometimes perform sub-optimally when serially correlated data exists [28]. The equal weighting of historical and current data may hinder detection sensitivity.

To overcome this problem, a modified EWMA control chart was presented, incorporating additional constants to focus on recent observations rather than historical ones. This approach has shown superior performance, especially when applied to data violating normality assumptions, with increased ARL performance compared to traditional EWMA control charts [14,29–32]. The revised charts have also shown excellent results when applied to real-world or industrial data sets, highlighting the practical value of the charts [33–36]. Notably, the modified EWMA chart surpasses the customary EWMA chart, according to multiple researchers, in detecting small process shifts, offering lower ARL_1 values and enhanced responsiveness in autocorrelated or non-normal environments.

This study proposes a novel modification of the EWMA control chart. We hypothesize that it will exhibit superior properties, especially in its capability to perceive minor deviations in the procedure more efficiently and achieve lower ARL. Using the second-type Fredholm integral equation, we deduce an explicit formula for the two-sided ARL to detect mean changes in seasonal regressive moving average ($SARMA(1,1)_L$) processes with exponential white noise. This particular model is selected because $SARMA(1,1)_L$ effectively captures both short-term autocorrelation and seasonal patterns commonly observed in real-world environmental and industrial processes, making it a realistic and practically relevant test case for evaluating control chart performance. The Gauss-Legendre quadrature is used as an efficient and accurate method to compare the proposed formula with the NIE approach. Finally, for the numerical integral, we validate the execution of our proposed control chart by applying it to rainfall data from Thailand, demonstrating its practical utility in monitoring environmental processes.

2 Qualities of Different EWMA Control Charts

Descriptions of the standard and modified Exponentially Weighted Moving Average (EWMA) control chart attributes appear within subsequent subsections. Modified EWMA charts provide increased efficiency by tackling autocorrelation and procedure-specific properties, whereas standard EWMA charts are useful for identifying negligible changes in procedure means.

2.1 The Standard EWMA Control Chart

The standard EWMA control chart allows negligible shifts to be distinguished in the procedure mean, which is described below:

$$Z_t = (1-\lambda)\, Z_{t-1} + \lambda Y_t;\ \ t = 1, 2, 3, \ldots, \tag{1}$$

in which Z_t indicates the EWMA statistic, Y_t represents the succession of the SARMA(1,1)$_L$ process with exponential white noise, while $0 < \lambda \leq 1$ serves as an exponential smoothing parameter.

The control chart indicates an out-of-control condition when the upper control limit (UCL) or lower control limit (LCL) is breached by the EWMA statistic. The stopping time τ_b reveals the first time point at which this occurs and can be written as:

$$\tau_b = \inf\left\{t > 0; Z_t < a \text{ or } Z_t > b\right\}\ , \tag{2}$$

in which here a represents the LCL and b represents the UCL. It is then possible to evaluate the ARL for the SARMA(1,1)$_L$ process on the standard EWMA control chart, which has a starting value ($Z_0 = u$). A function $L(u)$ is distinguished as

$$L(u) = \text{ARL} = E_\infty(\tau_b) \geq T, Z_0 = u\,, \tag{3}$$

in which the value of T is fixed (preferably large), and $E_\infty(.)$ represents the probability when it is postulated that the observations ε_t are distributed as $F(y_t, \alpha)$.

For the standard EWMA control chart, it is possible to express the mean and the variance as follows:

$$E(Z_t) = \mu\,, \tag{4}$$

and

$$Var(Z_t) = \left(\frac{\lambda}{2-\lambda}\right)\sigma^2. \tag{5}$$

In the case of the control limit (CL = μ_0), the standard EWMA control chart has the UCL and LCL as specified below:

$$\text{LCL, UCL} = \mu_0 \pm L_1\sigma\sqrt{\frac{\lambda}{(2-\lambda)}}, \tag{6}$$

in which μ_0 signifies the target mean, σ indicates the standard deviation of the process, and L_1 represents a multiplier that characterizes the control limits' width.

2.2 The Modified EWMA Control Chart

Khan et al. [14] improved an adapted EWMA indicator initially suggested by Patel and Divecha [15] by presenting a modernized EWMA control chart. This improved approach incorporates both historical and current process data, with the modified statistic expressed below:

$$M_t = (1-\lambda)\, M_{t-1} + \lambda Y_t + c\,(Y_t - Y_{t-1})\,; t = 1, 2, 3, \ldots, \tag{7}$$

in which M_t represents the modified EWMA statistic, M_t shows the succession of the SARMA$(1,1)_{\mathrm{L}}$ procedure with exponential white noise, λ serves as an exponential smoothing parameter $(0 < \lambda \leq 1)$, while c is a constant $(c > 0)$. Meanwhile, τ_h indicates the stopping time, which reveals the first time point at which this occurs in the case of the modified EWMA control chart, and is expressed in the form of

$$\tau_h = \inf\{t > 0; M_t < g \text{ or } M_t > h\}, \tag{8}$$

in which the LCL is shown as g and the UCL is given as h. The ARL for the SARMA$(1,1)_{\mathrm{L}}$ process on the modified EWMA control chart with an initial value $(M_0 = u)$ can then be evaluated. Now, we characterize the function $G(u)$ as

$$\mathrm{ARL} = G(u) = E_\infty(\tau_h) \geq T, M_0 = u, \tag{9}$$

in which the value of T is fixed, and $E_\infty(.)$ represents the expected value, assuming that the observations ε_t are distributed as $F(y_t, \alpha)$.

The modified EWMA control chart has mean and variance expressed as shown below:

$$E(M_t) = \mu\ , \tag{10}$$

and

$$Var(M_t) = \frac{\left(\lambda + 2\lambda c + 2c^2\right)\sigma^2}{(2-\lambda)}. \tag{11}$$

In the case of the control limit $(\mathrm{CL} = \mu_0)$, the modified EWMA control has the UCL and LCL for which can be determined using the equations below.

$$\mathrm{LCL, UCL} = \mu_0 \pm L_1\sigma\sqrt{\frac{(\lambda + 2\lambda c + 2c^2)}{(2-\lambda)}}, \tag{12}$$

where L_2 is a multiplier that distinguishes the control limits' width.

3 Analytical Derivation of Two-Sided ARL for SARMA$(1,1)_{\mathrm{L}}$ Process on the Modified EWMA Chart

The SARMA$(1,1)_{\mathrm{L}}$ procedure is particularly effective for applications where data shows periodicity, such as in climatology and economics, and is commonly used to create control charts that monitor shifts and anomalies in seasonal time series data. It is characterized by

$$Y_t = \mu + \phi Y_{t-L} + \varepsilon_t - \theta\varepsilon_{t-L}; t = 1, 2, 3, \ldots, \tag{13}$$

in which μ serves as a constant $(\mu \geq 0)$, ϕ is the autoregressive coefficient, θ is the moving average coefficient, ε_t represents independent and identically distributed (iid) observations from an exponential distribution $(\varepsilon_t \sim Exp(\beta))$, while the starting value ε_{t-L} is normally set to the mean of the procedure, and the initial value for the SARMA$(1,1)_{\mathrm{L}}$ process is $Y_{t-L} = 1$.

3.1 The Explicit Formula

The specific formulae for determining the ARL of the modified EWMA control chart for SARMA(1,1)$_L$ process are derived as follows:

$$M_t = (1-\lambda) M_{t-1} + (\lambda + c)(\mu + \phi Y_{t-L} - \theta \varepsilon_{t-L}) + (\lambda + c)\varepsilon_t - cY_{t-1}.$$

At $t = 1$, using the initial value $M_0 = u$, the expression becomes:

$$M_1 = (1-\lambda) u + (\lambda + c)(\mu + \phi Y_{t-L} - \theta \varepsilon_{t-L}) + (\lambda + c)\varepsilon_1 - cY_0.$$

If ε_1 is the in-control limit for M_1, then $g \le M_1 \le h$. Then for the function $G(u)$

$$G(u) = 1 + \int G(M_1) f(\varepsilon_1) d(\varepsilon_1). \tag{14}$$

Eq. (14) is a Fredholm integral equation of the second kind [21], so accordingly, it is possible to rewrite $G(u)$ in the form of

$$G(u) = 1 + \int_g^h G\{(1-\lambda) u + (\lambda + c)(\mu + \phi Y_{t-L} - \theta \varepsilon_{t-L}) - cY_{t-1} + (\lambda + c) y\} f(y) dy.$$

Let $w = (1-\lambda) u + (\lambda + c)(\mu + \phi Y_{t-L} - \theta \varepsilon_{t-L}) - cY_{t-1} + (\lambda + c) y$.

By substituting a new variable in the integral, the integral equation acquired is shown as follows:

$$G(u) = 1 + \frac{1}{\lambda + c} \int_g^h G(w) f\left\{\frac{w - (1-\lambda) u}{\lambda + c} + \frac{cY_{t-1}}{\lambda + c} - (\mu + \phi Y_{t-L} - \theta \varepsilon_{t-L})\right\} dw. \tag{15}$$

If $\varepsilon_t \sim Exp(\beta)$ the $f(y) = \frac{1}{\beta_0} e^{\frac{-y}{\beta_0}}$; $y \ge 0$. Accordingly, Eq. (15) can be rewritten as:

$$G(u) = 1 + \frac{1}{\lambda + c} \int_g^h G(w) \frac{1}{\beta_0} e^{-\frac{1}{\beta_0}\left\{\frac{w-(1-\lambda)u}{\lambda+c} + \frac{cY_{t-1}}{\lambda+c} - (\mu+\phi Y_{t-L} - \theta\varepsilon_{t-L})\right\}} dw. \tag{16}$$

Let function $C(u) = e^{\frac{(1-\lambda)u - cY_{t-1}}{\beta_0(\lambda+c)} + \frac{1}{\beta_0}(\mu+\phi Y_{t-L} - \theta\varepsilon_{t-L})}$. Consequently, Eq. (16) takes the form:

$$G(u) = 1 + \frac{C(u)}{\beta_0(\lambda+c)} \int_g^h G(w) e^{\frac{-w}{\beta_0(\lambda+c)}} dw; g \le u \le h.$$

Let $B = \int_g^h G(w) e^{\frac{-w}{\beta_0(\lambda+c)}} dw$, then $G(u) = 1 + \frac{C(u)}{\beta_0(\lambda+c)} \cdot B$. Consequently, we obtain

$$G(u) = 1 + \frac{1}{\beta_0(\lambda + c)} e^{\frac{(1-\lambda)u - cY_{t-1}}{\beta_0(\lambda+c)} + \frac{1}{\beta_0}(\mu+\phi Y_{t-L} - \theta\varepsilon_{t-L})} \cdot B. \tag{17}$$

When solved in the case of constant B from Eq. (17), the result is

$$B = \int_g^h G(w) e^{\frac{-w}{\beta_0(\lambda+c)}} dw = \frac{-\beta_0(\lambda+c)\left(e^{\frac{-h}{\beta_0(\lambda+c)}} - e^{\frac{-g}{\beta_0(\lambda+c)}}\right)}{1 + \frac{e^{\frac{-cY_{t-1}}{\beta_0(\lambda+c)} + \frac{1}{\beta_0}(\mu+\phi Y_{t-L} - \theta\varepsilon_{t-L})}}{\lambda}\left(e^{\frac{-\lambda h}{\beta_0(\lambda+c)}} - e^{\frac{-\lambda g}{\beta_0(\lambda+c)}}\right)}.$$

By substituting constant B into Eq. (17), we derive

$$G(u) = 1 + \frac{e^{\frac{(1-\lambda)u - cY_{t-1}}{\beta_0(\lambda+c)} + \frac{1}{\beta_0}(\mu+\phi Y_{t-L} - \theta\varepsilon_{t-L})}}{\beta_0(\lambda + c)} \cdot \left(\frac{-\beta_0(\lambda + c)\left(e^{\frac{-h}{\beta_0(\lambda+c)}} - e^{\frac{-g}{\beta_0(\lambda+c)}}\right)}{1 + \frac{e^{\frac{-cY_{t-1}}{\beta_0(\lambda+c)} + \frac{1}{\beta_0}(\mu+\phi Y_{t-L} - \theta\varepsilon_{t-L})}}{\lambda}\left(e^{\frac{-\lambda h}{\beta_0(\lambda+c)}} - e^{\frac{-\lambda g}{\beta_0(\lambda+c)}}\right)}\right). \tag{18}$$

Hence, the Fredholm integral equation of the second kind from Eq. (18) can describe the explicit formulas for the 2-sided ARL of the SARMA(1,1)$_L$ processes when examined by the modified EWMA control chart. The formulation can be simplified and expressed in a closed form as:

$$ARL = 1 - \frac{\lambda e^{\frac{(1-\lambda)u}{\beta_0(\lambda+c)}}\left[e^{\frac{-h}{\beta_0(\lambda+c)}} - e^{\frac{-g}{\beta_0(\lambda+c)}}\right]}{\lambda e^{\frac{cY_{t-1}}{\beta_0(\lambda+c)} + \frac{-\mu-\phi Y_{t-L}+\theta\varepsilon_{t-L}}{\beta_0}} + \left[e^{\frac{-\lambda h}{\beta_0(\lambda+c)}} - e^{\frac{-\lambda g}{\beta_0(\lambda+c)}}\right]}. \tag{19}$$

3.2 Presence and Distinctiveness of Explicit Formula

This study exhibits the presence and distinctiveness of the resolution to the integral equation in Eq. (16). Initially, this is expressed as

$$T(G(u)) = 1 + \frac{1}{\lambda + c}\int_g^h G(w)\frac{1}{\beta_0}e^{-\frac{1}{\beta_0}\left\{\frac{w-(1-\lambda)u}{\lambda+c} + \frac{cY_{t-1}}{\lambda+c} - (\mu+\phi Y_{t-L}-\theta\varepsilon_{t-L})\right\}}dw. \tag{20}$$

Theorem 1. (*Banach's fixed-point theorem* [37]) *Where C[g, h] is the set comprising all continuous functions on the complete metric (X, d), under the assumption that T: X →X is a contraction mapping with the contraction constant* $r; 0 \le r < 1$; i.e., $\|T(G_1) - T(G_2)\| \le r\|G_1 - G_2\|\ \forall G_1, G_2 \in X$. *Subsequently,* $G(.) \in X$ *can be considered unique at* $T(G(u)) = G(u)$*; that is, it has a unique fixed point in X, indicating that a unique solution exists at this point.*

Proof of Theorem 1. To demonstrate that T characterized in Eq. (17) is a contraction mapping for $G_1, G_2 \in C[g, h]$, the inequality $\|T(G_1) - T(G_2)\| \le r\|G_1 - G_2\|\ \forall G_1, G_2 \in C(l, r)$ is applied with $0 \le r < 1$. Consider Eqs. (16) and (20), so that

$$\begin{aligned}
\|T(G_1) - T(G_2)\|_\infty &= \sup_{u\in[g,h]}\left|\frac{C(u)}{\beta_0(\lambda+c)}\int_g^h (G_1(w) - G_2(w))\, e^{\frac{-w}{\beta_0(\lambda+c)}}dw\right| \\
&\le \sup_{u\in[g,h]}\left|\|G_1 - G_2\|_\infty C(u)\left(e^{\frac{-g}{\beta_0(\lambda+c)}} - e^{\frac{-h}{\beta_0(\lambda+c)}}\right)\right| \\
&= \|G_1 - G_2\|_\infty \left|e^{\frac{-g}{\beta_0(\lambda+c)}} - e^{\frac{-h}{\beta_0(\lambda+c)}}\right| \sup_{u\in[g,h]}|C(u)| \\
&\le r\|G_1 - G_2\|_\infty,
\end{aligned}$$

where $r = \left|e^{\frac{-g}{\beta_0(\lambda+c)}} - e^{\frac{-h}{\beta_0(\lambda+c)}}\right| \sup_{u\in[g,h]}|C(u)|$ and $C(u) = e^{-\frac{1}{\beta_0}\left\{\frac{w-(1-\lambda)u}{\lambda+c} + \frac{cY_{t-1}}{\lambda+c} - (\mu+\phi Y_{t-L}-\theta\varepsilon_{t-L})\right\}}; 0 \le r < 1.$

Thus, this study confirms the presence and exclusivity of the solution through the application of Banach's fixed-point theorem. □

4 The NIE for the ARL of SARMA(1,1)$_L$ Process on the Modified EWMA Control Chart

Often implemented with a variety of quadrature rules, including midpoint, trapezoidal, Simpson's rule, and Gauss-Legendre, the NIE technique is frequently engaged to assess the ARL. Each of these methods produces ARL values that are highly similar to one another [38]. The interval is determined when utilizing the midpoint, trapezoidal, and Simpson's rules to solve the issues involved in integrating a function over the interval. However, it becomes interminable when applying the Gauss-Legendre parameter [39]. Thus, this research assessed the ARL by means of the Gauss-Legendre rule. The quadrature formula can be applied to estimate an integral equation of the second kind to apply to the ARL on the modified EWMA control

chart in the case of the SARMA(1,1)$_L$ procedure in Eq. (18). The Gauss-Legendre quadrature directive is utilized below:

Given

$$f\left(a_j\right) = f\left\{\frac{a_j - (1-\lambda)\, a_i}{(\lambda + c)} + \frac{c Y_{t-1}}{(\lambda + c)} - \left(\mu + \phi Y_{t-L} - \theta \varepsilon_{t-L}\right)\right\}. \tag{21}$$

The calculation for the integral of Eq. (21) is as follows.

$$f\left(a_j\right) = \int_g^h G\left(w\right) f\left(w\right) dw \approx \sum_{j=1}^{m} w_j f\left(a_j\right) \ , \tag{22}$$

in which $a_j = \frac{h-g}{m}\left(j - 1/2\right) + g$, while $w_j = \frac{h-g}{m}; j = 1, 2, \ldots, m$.

By applying the Gauss-Legendre quadrature formula, a numerical approximation $\tilde{G}\left(u\right)$ is obtained for the integral equation by solving the linear equations below:

$$\sum_{j=1}^{m} w_j \tilde{G}\left(a_j\right) f\left\{\frac{a_j - (1-\lambda)\, u}{(\lambda + c)} + \frac{c Y_{t-1}}{(\lambda + c)} - \left(\mu + \phi Y_{t-L} - \theta \varepsilon_{t-L}\right)\right\}. \tag{23}$$

5 Results of Comparing the Accuracy of Explicit Formula and NIE Methods

Specifics are given in this section concerning a simulation assessing the efficacy of the NIE approach and explicit formulas in gauging the ARL for the ARMA(1,1)$_L$ procedure for the modified EWMA control chart suggested in this study. The study was performed with parameters set as follows: λ = 0.05 or 0.15; constant c = 0.5, and 2; in-control parameter β_0 = 1; and a range of shift sizes, specifically 0.01, 0.03, 0.05, 0.10, 0.30, 0.50, and 1.00 for ARL$_0$ values of 370 and 500. The detailed programming algorithm and computational steps used for the ARL calculation are provided in Appendix A. To measure the accuracy, the percentage accuracy was calculated as follows:

$$\%ACC = 100 - \frac{\left|G\left(u\right) - \tilde{G}\left(u\right)\right|}{G\left(u\right)} \times 100. \tag{24}$$

in which $\tilde{G}\left(u\right)$ and $G\left(u\right)$ indicate the respective value for ARL under the NIE and explicit formulas approaches. The accuracy exceeded 95 percent, suggesting strong agreement between ARL values obtained through the NIE method and those acquired from explicit formulas.

Eqs. (18) and (23) were employed to derive the SARMA(1,1)$_L$ process ARL with exponential white noise under the modified EWMA control chart. All computations, including both the numerical integration (NIE method with 1000 iterations) and the evaluation of the explicit ARL formulas, were performed using a computer equipped with an Intel(R) Core(TM) i5-8265U CPU @ 1.60 GHz 1.80 GHz and 8.00 GB RAM, using Mathematica, ensuring consistency, precision, and computational efficiency. The resulting ARL values are presented in Tables 1 and 2.

Table 1: Two-sided assessment of ARL determined using explicit formula and NIE methods for SARMA(1,1)$_3$ process on the modified EWMA control chart with μ = 2, ϕ = 0.3, θ = 0.6 for ARL$_0$ = 370

c	*λ*	*g*	*h*	Shift	Explicit	Time	NIE	Time	%ACC
				0.00	370.064567	<0.001	370.064561	8.563	100%
				0.01	117.490572	<0.001	117.490570	9.687	100%
				0.03	49.082966	<0.001	49.082966	8.594	100%

(Continued)

Table 1 (continued)

c	*λ*	*g*	*h*	Shift	Explicit	Time	NIE	Time	%ACC
0.5	0.1	0.1	0.359789	0.05	30.745438	<0.001	30.745438	8.000	100%
				0.10	15.650593	<0.001	15.650593	7.906	100%
				0.30	5.157724	<0.001	5.157724	8.609	100%
				0.50	3.180012	<0.001	3.180012	8.782	100%
				1.00	1.869686	<0.001	1.869686	8.141	100%
	0.15	0.1	0.368459	0.00	370.140406	<0.001	370.140396	6.422	100%
				0.01	103.890983	<0.001	103.890981	8.015	100%
				0.03	42.261026	<0.001	42.261026	8.500	100%
				0.05	26.378659	<0.001	26.378659	8.625	100%
				0.10	13.488829	<0.001	13.488829	8.109	100%
				0.30	4.594950	<0.001	4.594950	7.813	100%
				0.50	2.909300	<0.001	2.909300`	7.812	100%
				1.00	1.778229	<0.001	1.778229	7.890	100%
2	0.1	0.1	1.12025	0.00	370.355205	<0.001	370.355190	7.593	100%
				0.01	59.107585	<0.001	59.107585	8.937	100%
				0.03	22.507135	<0.001	22.507135	8.438	100%
				0.05	14.132743	<0.001	14.132743	8.235	100%
				0.10	7.589736	<0.001	7.589736	7.890	100%
				0.30	3.119988	<0.001	3.119988	8.422	100%
				0.50	2.230702	<0.001	2.230702	8.000	100%
				1.00	1.581505	<0.001	1.581505	7.812	100%
	0.15	0.1	1.13606	0.00	370.070685	<0.001	370.070657	8.469	100%
				0.01	58.081755	<0.001	58.081754	8.172	100%
				0.03	22.090851	<0.001	22.090850	8.812	100%
				0.05	13.875962	<0.001	13.875962	8.016	100%
				0.10	7.462442	<0.001	7.462442	8.766	100%
				0.30	3.082496	<0.001	3.082496	9.406	100%
				0.50	2.210542	<0.001	2.210542	7.781	100%
				1.00	1.573214	<0.001	1.573214	7.906	100%

Table 2: Two-sided evaluation of ARL acquired on the basis of explicit formula and NIE approaches for SARMA(1,1)$_4$ procedure on the modified EWMA control chart, whereby $\mu = 2, \phi = -0.2, \theta = -0.4$ for $ARL_0 = 500$

c	*λ*	*g*	*h*	Shift	Explicit	Time	NIE	Time	%ACC
0.5	0.1	0.1	0.256503	0.00	500.130483	<0.001	500.130480	8.672	100%
				0.01	112.362512	<0.001	112.362511	8.547	100%
				0.03	43.385365	<0.001	43.385365	8.421	100%
				0.05	26.587779	<0.001	26.587778	7.797	100%
				0.10	13.259192	<0.001	13.259192	7.282	100%
				0.30	4.305703	<0.001	4.305703	7.265	100%
				0.50	2.676413	<0.001	2.676413	8.844	100%
				1.00	1.632659	<0.001	1.632659	7.672	100%
	0.15	0.1	0.26109	0.00	500.232124	<0.001	500.232117	7.392	100%
				0.01	97.567592	<0.001	97.567591	9.000	100%
				0.03	36.993062	<0.001	36.993062	8.781	100%
				0.05	22.661447	<0.001	22.661447	8.531	100%
				0.10	11.393638	<0.001	11.393638	8.422	100%
				0.30	3.848109	<0.001	3.848109	7.875	100%
				0.50	2.463609	<0.001	2.463609	8.671	100%
				1.00	1.564449	<0.001	1.564449	8.188	100%

(Continued)

Table 2 (continued)

c	*λ*	*g*	*h*	Shift	Explicit	Time	NIE	Time	%ACC
2	0.1	0.1	0.713274	0.00	500.026242	<0.001	500.026233	7.797	100%
				0.01	52.610598	<0.001	52.610598	9.938	100%
				0.03	19.272541	<0.001	19.272541	8.156	100%
				0.05	12.005343	<0.001	12.005343	8.297	100%
				0.10	6.420518	<0.001	6.420518	7.734	100%
				0.30	2.668152	<0.001	2.668152	9.468	100%
				0.50	1.938164	<0.001	1.938164	8.516	100%
				1.00	1.420060	<0.001	1.420060	9.297	100%
	0.15	0.1	0.719828	0.00	500.299402	<0.001	500.299385	8.672	100%
				0.01	51.390406	<0.001	51.390405	9.282	100%
				0.03	18.813729	<0.001	18.813728	8.203	100%
				0.05	11.727934	<0.001	11.727934	8.125	100%
				0.10	8.630487	<0.001	8.630487	8.609	100%
				0.30	6.285898	<0.001	6.285898	8.516	100%
				0.50	2.629906	<0.001	2.629906	7.500	100%
				1.00	1.918023	<0.001	1.918023	8.125	100%

The two-sided evaluation of ARL values calculated by means of the suggested explicit formulas completely corresponds with those acquired by applying the numerical integral equation (NIE) procedure, as shown in Tables 1 and 2. This consistency confirms the mathematical accuracy and validity of the closed-form solutions derived in this study. Specifically, the numerical ARL approximations from both approaches exhibited a 100% match across all test scenarios, ensuring that the explicit formulation introduced no loss in precision.

Although both methods yield identical ARL results, their computational efficiency differs greatly. The NIE method takes about 7–9 s per evaluation due to complex numerical procedures, while the explicit formulas produce results in under 0.001 s—over 7000 times faster. This efficiency makes the proposed method highly suitable for real-time monitoring and large-scale applications in automated statistical process control.

6 Evaluating Control Chart Performance via Explicit ARL Formula

The current research employed an extended analysis to evaluate a number of different control charts to compare their efficiency to that of the original EWMA control chart. To gauge their efficacy, performance metrics including Performance Comparison Index (PCI) and Average Extra Quadratic Loss (AEQL) were employed [40].

$$AEQL = \frac{1}{\Delta}\sum_{\delta}\delta^2 \times ARL\ , \tag{25}$$

in which δ symbolizes a specific alteration to the process and Δ quantifies the divisions between the initial and final states. In this research, $\delta = 8$ is established by the interval range. Control charts with lower AEQL values are deemed to be more efficient.

The PCI metric evaluates the AEQL for a specific chart and compares it to the most suitable chart for which the AEQL value is lowest, so that the control chart efficiency can be determined. The PCI can be mathematically represented as:

$$PCI = \frac{AEQL}{AEQL_{smallest}}. \tag{26}$$

where the value for PCI equals 1, this indicates the most efficient control chart, while values above 1 suggest lower efficiency.

For the two-sided ARL comparison of the SARMA(1,1)$_L$ process on standard and modified EWMA control charts, parameters were set as follows: target ARL$_0$ = 370, and 500; smoothing parameters λ = 0.1 or 0.15; in-control parameter β_0 = 1, while a range of shift sizes are employed including 0.01, 0.03, 0.05, 0.07, 0.10, 0.30, 0.50, 0.70, and 1.00. In the case of the modified EWMA control chart, constant parameters c = 0.5, and 2 were utilized. Tables 3–6 present a detailed assessment comparing the modified EWMA control chart detection capabilities with those of the traditional EWMA chart for various SARMA(1,1)$_L$ processes with distinct parameter settings, highlighting the advantages of the modified chart.

Table 3: Two-sided assessment of the SARMA(1,1)$_3$ process ARL on standard, and modified EWMA control charts whereby μ = 5, ϕ = 0.4, θ = 0.6 for ARL$_0$ = 370

λ	Shift	EWMA	Modified	
			$c = 0.5$	$c = 2$
		(a = 0.11, b = 0.1101004)	(g = 0.11, h = 0.1214662)	(g = 0.11, h = 0.154901)
	0.00	370.2461	370.3723	370.2244
	0.01	321.2402	61.9890	28.1248
	0.03	244.0842	22.6682	10.1702
0.1	0.05	187.6294	13.6290	6.3628
	0.10	101.7847	6.6514	3.4779
	0.30	14.8962	2.2244	1.6143
	0.50	4.2300	1.5209	1.2900
	1.00	1.2888	1.1433	1.0948
AEQL		0.678	0.231	0.203
PCI		3.338	1.139	1.000
		(a = 0.12, b = 0.120998)	(g = 0.12, h = 0.1317846)	(g = 0.12, h = 0.1651328)
	0.00	370.3913	370.1106	370.3834
	0.01	292.9485	52.9018	27.2288
	0.03	196.1949	19.1483	9.8557
0.15	0.05	139.6380	11.5622	6.1791
	0.10	69.8296	5.7422	3.3948
	0.30	11.6510	2.0469	1.5954
	0.50	4.0955	1.4518	1.2816
	1.00	1.4322	1.1273	1.0923
AEQL		0.595	0.223	0.202
PCI		2.942	1.103	1.000

Table 4: Two-sided assessment of the SARMA(1,1)$_4$ procedure ARL on standard, and modified EWMA control charts whereby $\mu = 5, \phi = -0.7, \theta = -0.3$ for $ARL_0 = 370$

λ	Shift	EWMA	Modified	
			c=0.5	c=2
		($a = 0.13, b = 0.1301467$)	($g = 0.13, h = 0.1440591$)	($g = 0.13, h = 0.1849099$)
	0.00	370.3928	370.35513	370.3512
	0.01	332.3112	62.5874	28.9626
	0.03	246.3296	22.9608	10.4881
0.1	0.05	187.6294	13.6290	6.3628
	0.10	101.7847	6.7799	3.5838
	0.30	16.0269	2.2799	1.6526
	0.50	4.6290	1.5543	1.3128
	1.00	1.3461	1.1575	1.1051
AEQL		0.716	0.235	0.206
PCI		3.476	1.142	1.000
		($a = 0.14, b = 0.141283$)	($g = 0.14, h = 0.1544682$)	($g = 0.14, h = 0.1952237$)
	0.00	370.4229	370.2368	370.2395
	0.01	291.1626	53.5969	28.0586
	0.03	193.7664	19.4604	10.1695
0.15	0.05	137.6075	11.7732	6.3756
	0.10	68.9394	5.8670	3.4989
	0.30	11.8002	2.0978	1.6329
	0.50	4.2241	1.4822	1.3040
	1.00	1.4726	1.1402	1.1025
AEQL		0.603	0.226	0.205
PCI		2.947	1.105	1.000

Table 5: Two-sided evaluation of the SARMA(1,1)$_3$ procedure ARL on standard, and modified EWMA control charts whereby $\mu = 4, \phi = 0.8, \theta = 0.7$ for $ARL_0 = 500$

λ	Shift	EWMA	Modified	
			$c = 0.5$	$c = 2$
		($a = 0.15, b = 0.1503703$)	($g = 0.15, h = 0.1733404$)	($g = 0.15, h = 0.2407904$)
	0.00	500.2356	500.0991	500.2841
	0.01	436.7038	70.0913	32.3918
	0.03	336.0106	25.2338	11.6068
0.1	0.05	261.6052	15.1687	7.2366
	0.10	146.4795	7.4394	3.9279
	0.30	23.6909	2.4907	1.7716
	0.50	6.8298	1.6707	1.3835
	1.00	1.6192	1.2044	1.1376

(Continued)

Table 5 (continued)

λ	Shift	EWMA	Modified	
			$c = 0.5$	$c = 2$
AEQL		0.990	0.249	0.214
PCI		4.623	1.160	1.000
		($a = 0.16, b = 0.16237$)	($g = 0.16, h = 0.1840468$)	($g = 0.16, h = 0.2513836$)
	0.00	500.0805	500.2214	500.2272
	0.01	377.0757	59.8703	31.3892
	0.03	239.3496	21.3902	11.2579
0.15	0.05	165.8611	12.9131	7.0321
	0.10	81.1438	6.4346	3.8340
	0.30	14.0115	2.2815	1.7490
	0.50	5.0504	1.5848	1.3729
	1.00	1.6463	1.1822	1.1343
AEQL		0.706	0.238	0.213
PCI		3.315	1.118	1.000

Table 6: Two-sided evaluation of the SARMA(1,1)$_4$ procedure ARL on standard, and modified EWMA control charts whereby $\mu = 4, \phi = -0.9, \theta = 0.8$ for ARL$_0 = 500$

λ	Shift	EWMA	Modified	
			$c = 0.5$	$c = 2$
		($a = 0.17, b = 0.1705326$)	($g = 0.17, h = 0.1986225$)	($g = 0.17, h = 0.2810548$)
	0.00	500.2536	500.1516	500.2241
	0.01	437.7328	71.1029	33.5322
	0.03	388.3995	25.6855	12.0327
0.1	0.05	264.7337	15.4735	7.5026
	0.10	150.0238	7.6194	4.0690
	0.30	25.3065	2.5655	1.8236
	0.50	7.4746	1.7167	1.4154
	1.00	1.7318	1.2252	1.1531
AEQL		0.7143	0.2527	0.2222
PCI		3.2548	1.1513	1.0125
		($a = 0.18, b = 0.183016$)	($g = 0.18, h = 0.2095304$)	($g = 0.18, h = 0.2918554$)
	0.00	500.0696	500.1078	500.2086
	0.01	373.6679	60.9542	32.5226
	0.03	235.2074	21.8490	11.6795
0.15	0.05	162.5503	13.2151	7.2951
	0.10	79.6628	6.6067	3.9732
	0.30	14.1189	2.3502	1.8001

(Continued)

Table 6 (continued)

	0.50	5.1919	1.6267	1.4043
	1.00	1.7013	1.2013	1.1495
AEQL		5.1979	0.2473	0.2240
PCI		23.4531	1.1159	1.0109

Table 3: For the SARMA(1,1)$_3$ process with parameters $\mu = 5, \phi = 0.4$, and $\theta = 0.6$ set at $\lambda = 0.1$ and $\lambda = 0.15$ and target $ARL_0 = 370$, the modified EWMA control chart consistently demonstrates lower out-of-control values for ARL than the traditional chart for all different shift sizes and c values. The explicit formulas applied with the modified chart not only reduced ARL but also achieved a Performance Comparison Index (PCI) of 1.000 at $c = 2$. The findings indicate that increasing λ values from 0.1 to 0.15 further improved detection rates, showing that the responsiveness of the modified chart to process shifts is heightened with higher λ values.

Table 4: The SARMA(1,1)$_4$ process with parameters $\mu = 5, \phi = -0.7$ and $\theta = -0.3$ similarly shows improved ARL outcomes for the modified EWMA control chart under identical λ and ARL_0 values. The ARL of the modified chart consistently remained below that of the conventional EWMA across every shift size. A PCI equal to 1.000 was reached at $c = 3$, and increasing λ further decreased ARLs, confirming enhanced detection ability, especially in scenarios of smaller shifts.

Table 5: With the SARMA(1,1)$_3$ process, configured parameters $\mu = 4, \phi = 0.8$, and $\theta = 0.7$, and a target $ARL_0 = 500$, the modified EWMA chart consistently offered superior performance to the standard EWMA chart, achieving lower ARLs across all examined shift sizes. The explicit formulas enabled the modified EWMA chart to reach a Performance Comparison Index (PCI) of 1.000 at $c = 2$, indicating optimal detection efficiency in this setting. Additionally, when the exponential smoothing parameter λ was increased, the ARLs were further reduced, highlighting the enhanced sensitivity of the chart to distinguishing process shifts in cases with higher target ARL_0 values.

Table 6: For the SARMA(1,1)$_4$ process, with parameters set as $\mu = 4, \phi = -0.9$, and $\theta = -0.8$ at a target ARL_0 of 500, the findings were consistent with those observed in earlier tables. The modified EWMA control chart demonstrated superior detection capabilities, achieving lower ARLs across all shift sizes and c values compared to the standard chart. Notably, the modified chart attained a Performance Comparison Index (PCI) of 1.000 at $c = 2$, and as the exponential smoothing parameter λ increased, further reductions in ARL were observed. These results underscore the robustness and efficiency associated with the modified EWMA chart in examining process mean shifts across a range of parameter settings. This indicates that the modified EWMA chart, particularly at higher smoothing levels and larger constant values, is highly effective for promptly identifying shifts in processes with substantial in-control ARLs, which is advantageous for monitoring systems requiring rapid response to minor to moderate shifts.

In analyzing the various configurations, the results showed that a higher constant multiplier value of $c = 2$ in combination with an exponential smoothing parameter of $\lambda = 0.15$ provided the lowest ARL values through all shift sizes and parameter settings in the modified EWMA control chart. This combination delivers significant improvements in the sensitivity of the modified EWMA, allowing it to perceive even minor process shifts more rapidly and reliably than the conventional EWMA chart.

The modified chart structure, incorporating both past and present data points through an optimized constant c and a relatively high λ value, further enhances its responsiveness, especially in situations where

immediate detection is critical. This setup allows the modified EWMA control chart to lower ARLs effectively, regardless of process shifts, underscoring its superior detection performance.

The advantages are particularly evident when applied to processes with high target ARL_0 value, such as $ARL_0 = 370$ or $ARL_0 = 500$, where minor to moderate shifts need prompt identification. The configuration of $c = 2$ and $\lambda = 0.15$ minimizes ARL values consistently, reflecting a design well-suited to high-sensitivity monitoring in a variety of real-world applications. This makes it a powerful tool for maintaining process stability and quality control, ensuring that shifts are promptly flagged and addressed to uphold operational standards.

In summary, the choice of $c = 2$ and $\lambda = 0.15$ is optimal for the modified EWMA control chart to achieve high detection accuracy, demonstrating how optimized parameter tuning can offer significant improvements over traditional control charts in rigorous monitoring environments.

7 Real Data Analysis

Climate zones play a crucial role in shaping regional weather patterns, particularly in influencing rainfall distribution and the frequency of extreme weather events, such as flooding. In Thailand, the country's diverse topography and geographical location create a variety of climate zones, ranging from tropical savanna in the central regions to humid subtropical in the north and southwest. These distinct climate zones not only affect the amount and timing of rainfall but also contribute to the severity of floods, especially during the monsoon season.

Thailand experiences a tropical monsoon climate, with a marked rainy season from May to October. During this time, heavy rainfall often leads to flooding, particularly in low-lying areas and river basins. Monitoring rainfall patterns is therefore essential for effective disaster management and mitigation strategies, as excessive rainfall can have significant social, economic, and environmental impacts.

The objective of this section is to develop and implement an efficient rainfall monitoring system for Thailand, using statistical process control techniques. By analyzing historical rainfall data and applying advanced methods like the modified Exponentially Weighted Moving Average (EWMA) control chart, this investigation intends to distinguish trends and anomalies in rainfall patterns. This proactive approach will enhance understanding of climate variability and provide valuable insights for policymakers and local authorities, helping them improve flood preparedness and response strategies. The dataset used in this study comprises monthly average rainfall data for Thailand, derived from station-level measurements by the Meteorological Department using the Inverse Distance Weighted (IDW) spatial averaging method. The Box-Jenkins method was employed to test for autocorrelation in the data, while the t-statistic confirmed that the time-series data followed an $SARMA(1,1)_{12}$ process. The dataset spans from January 1970 to July 2023 [41], consisting of 644 observations, which were found to be autocorrelated and appropriate for analysis using the $SARMA(1,1)_{12}$ model. It is written as follows:

$$Y_t = 122.488 + 1.000 Y_{t-12} + 0.962 \varepsilon_{t-12} + \varepsilon_t \text{ where } \varepsilon_t \sim Exp\,(29.96)$$

The ARLs for the $SARMA(1,1)_{12}$ process of Thailand's average rainfall data were calculated employing both standard EWMA and modified EWMA control charts. The recommended exponential smoothing parameters for the modified EWMA control chart, $\lambda = 0.1$, and 0.15 and constant $c = 0.5$ for ARL0 = 370, and 500, were used. ARL results are presented in Tables 5 and 6 for in-control ARLs of 370 and 500, respectively. The evaluation of the ARLs was conducted employing explicit formulas for the EWMA control chart with lower control limits (LCLs) a and upper control limits (UCLs) b. The shift sizes are specified as 0.01, 0.03, 0.05, 0.07, 0.10, 0.30, 0.50, 0.70, 1.00, 2.00, 3.00, and 5.00.

As presented in Tables 7 and 8, the findings for ARL are in close alignment with the outcomes of the simulations, confirming that the proposed updated EWMA control chart outshines the original EWMA chart across an array of shift magnitudes and parameter values. Notably, the ability to rapidly detect changes in the means in the modified EWMA chart is particularly evident with larger shifts, underscoring its robust detection capabilities.

Table 7: Two-sided assessment of the ARL of the SARMA$(1,1)_{12}$ procedure for the mean rainfall of Thailand running on standard and modified EWMA control charts for $ARL_0 = 370$

Shift	$\lambda = 0.1$		$\lambda = 0.15$	
	EWMA (a = 0.13, b = 0.1802531)	**Modified EWMA (g = 0.13, h = 0.439121)**	**EWMA (a = 0.13, b = 0.2054356)**	**Modified EWMA (g = 0.13, h = 0.464407)**
0.00	370.1101	370.0037	370.3505	370.3354
0.01	249.0438	231.1471	241.2212	230.8057
0.03	150.6734	132.2225	142.2666	131.8072
0.05	108.0942	92.7136	100.9821	92.3620
0.07	84.3289	71.4540	78.3290	71.1587
0.10	63.4696	53.2397	58.6706	53.0048
0.30	24.1971	20.0277	22.2175	19.9320
0.50	15.1070	12.5338	13.8819	12.4747
0.70	11.0658	9.2245	10.1880	9.1821
1.00	7.9771	6.7041	7.3696	6.6747
2.00	4.3189	3.7271	4.0360	3.7133
3.00	3.0954	2.7320	2.9214	2.7234
5.00	2.1299	1.9449	2.0410	1.9403
AEQL	9.1703	8.1181	8.6668	8.0930
PCI	1.1331	1.0031	1.0709	1.0000

Table 8: Two-sided evaluation of the ARL of the SARMA$(1,1)_{12}$ procedure for the mean rainfall of Thailand running on standard and modified EWMA control charts for $ARL_0 = 500$

shift	$\lambda = 0.1$		$\lambda = 0.15$	
	EWMA (a = 0.12, b = 0.1702816)	**Modified EWMA (g = 0.12, h = 0.42933)**	**EWMA (a = 0.12, b = 0.21954722)**	**Modified EWMA (g = 0.12, h = 0.454624)**
0.00	500.3473	500.4866	500.3267	500.4975
0.01	302.2207	276.0930	290.5028	275.4187
0.03	168.8063	145.7862	158.1726	145.2245
0.05	117.2067	99.1778	108.7860	98.7470
0.07	89.8246	75.2294	82.9683	74.8845
0.10	66.5744	55.3047	61.2546	55.0408
0.30	24.6702	20.3100	22.5941	20.2093
0.50	15.3021	12.6425	14.0333	12.5812

(Continued)

Table 8 (continued)

shift	$\lambda = 0.1$		$\lambda = 0.15$	
	EWMA (a = 0.12, b = 0.1702816)	**Modified EWMA (g = 0.12, h = 0.42933)**	**EWMA (a = 0.12, b = 0.21954722)**	**Modified EWMA (g = 0.12, h = 0.454624)**
0.70	11.1758	9.2825	10.2717	9.2388
1.00	8.0378	6.7340	7.4147	6.7039
2.00	4.3388	3.7356	4.0502	3.7215
3.00	3.1060	2.7362	2.9288	2.7274
5.00	2.1346	1.9465	2.0443	1.9419
AEQL	9.2165	8.1408	8.7015	8.1152
PCI	1.1357	1.0032	1.0722	1.0000

This improved performance is particularly marked when using higher values for the constant, with a setting of $c = 2$ in particular achieving the lowest ARL values, emphasizing the rapid shift detection of the chart in processes with both large and small parameter settings. Additionally, when comparing smaller settings, a constant value of $c = 0.5$ was selected to directly compare the modified chart's performance against the standard EWMA, providing a baseline that highlights the modified chart's enhanced sensitivity even at lower parameter configurations.

Further, the results for λ values of 0.1 and 0.15 show slight differences, suggesting that while both settings enhance the chart's detection efficiency, subtle distinctions may influence detection speed, particularly in processes where the mean shift is subtle.

The modified EWMA chart's effectiveness is also validated through performance indices, including the Performance Comparison Index (PCI) and the Average Extra Quadratic Loss (AEQL). Achieving a PCI of 1.000, the modified chart demonstrates optimal performance, consistently minimizing detection delays and thus reducing potential loss associated with late shift identification. The high PCI scores, coupled with reduced ARLs, further confirm the suitability of the modified EWMA control chart as a reliable, adaptive instrument capable of maintaining rigorous process control across diverse settings.

The modified EWMA control chart performance suggested in this research is further established by applying it to examine and detect variations in average rainfall, showcasing its effectiveness in handling real-world data with seasonal patterns. Fig. 1 shows the control chart plotting average rainfall data over time, with control limits designed to signal potential shifts or anomalies. The efficacy of the modified EWMA chart is unmistakable, as it allows for early detection of deviations in rainfall patterns-whether unusually high, which may indicate potential flooding, or significantly low, which could signal drought conditions.

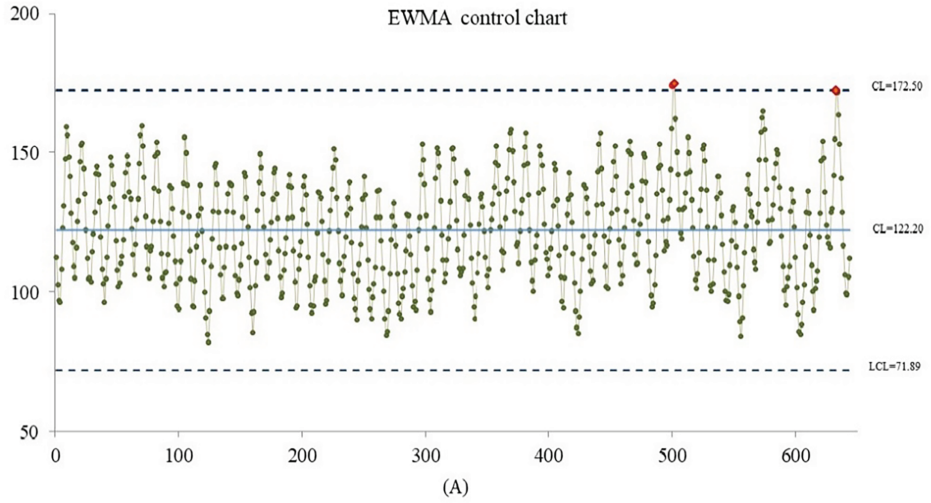

Figure 1: Mean shift detection of average rainfall from Thailand on the EWMA control chart

Fig. 1 illustrates the standard EWMA control chart in operation, detecting high rainfall anomalies at the 501st to 502nd observations and again at the 633rd observation (331.18 mm, close to the highest recorded average rainfall). However, it fails to capture earlier shifts in rainfall patterns, limiting its effectiveness in timely anomaly detection.

In contrast, Fig. 2 reveals the exceptional execution of the modified EWMA control chart, which detects abnormalities earlier and more accurately. It issues warning signals between the 632nd and 633rd observations for unusually high rainfall and promptly identifies the initial anomaly between the 6th and 8th to 9th observations, where estimated rainfall significantly exceeds the average. Moreover, the modified EWMA control chart effectively flags extremely high and low rainfall values surpassing control limits, including observation 488 (August 2010), which recorded the highest rainfall at 331.78 mm.

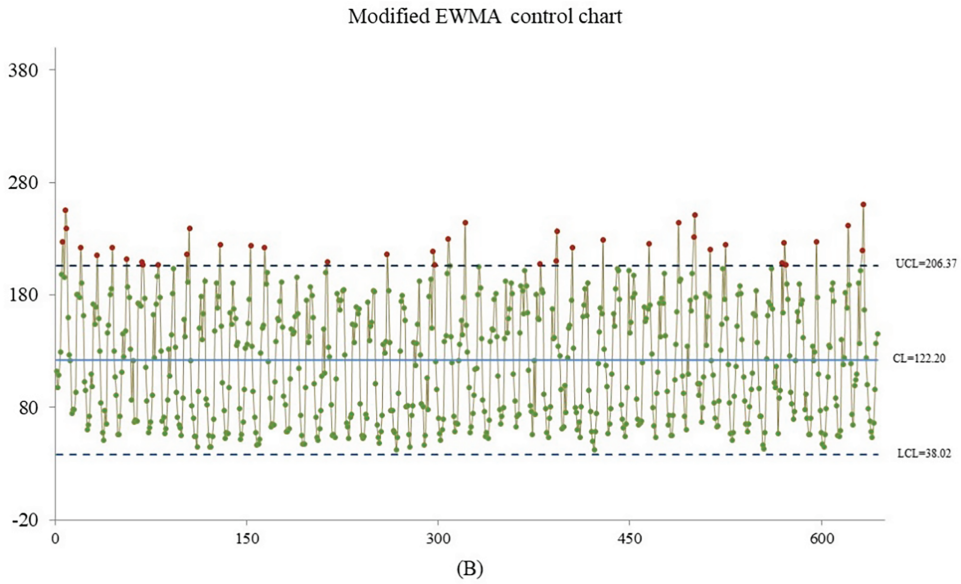

Figure 2: Mean shift detection of average rainfall from Thailand on the EWMA control chart

To summarize, utilizing statistical monitoring techniques in assessing rainfall patterns in Thailand is essential for managing the risks associated with climate variability and extreme weather events. By focusing on the relationships between climate zones, rainfall occurrences, and flooding, this study seeks to contribute valuable knowledge that can inform future climate adaptation efforts in the region.

8 Discussion

This modified EWMA control chart demonstrated notable improvements in distinguishing minor changes within autocorrelated data, particularly when applied to the SARMA$(1,1)_L$ process with exponential white noise. Using an approach of deriving two-sided ARL values via an explicit formula, validated by the NIE approach, this study showcased exceptional accuracy. Both methods yielded nearly identical ARL values, with the explicit formula providing a practical advantage by delivering results instantaneously, whereas the NIE method required 7–9 s per calculation. This efficiency makes the explicit formula highly suitable for real-time monitoring where rapid detection is essential.

When contrasted against the customary EWMA chart, further assessment of the performance of the modified EWMA chart revealed its dominance across various mean shift scenarios under out-of-control conditions, as shown by the consistently lower ARL_1 values for SARMA$(1,1)_3$ and SARMA$(1,1)_4$ processes. Tables 3–6 provide detailed comparisons of ARL outcomes, emphasizing the efficacy of the chart in perceiving shifts with an optimal Performance Comparison Index (PCI) of 1.000, achieved at a smoothing parameter (λ) equal to 0.15 while the constant (c) was 2. These findings illustrate that the modified EWMA control chart is extremely responsive and reliable in environments where the smallest of changes could have significant impacts.

Several previous studies have highlighted the functional benefits associated with the modified EWMA control chart under different configurations. Paichit and Peerajit [34] reported that with a smoothing parameter (λ) of 0.10, the modified EWMA chart offered negligibly superior performance to the standard EWMA chart by producing minor out-of-control ARL values, performing better than with λ = 0.05 and comparable to the findings of Supharakonsakun et al. [32]. In the study by Phanthuna et al. [36], a higher λ value of 0.20 demonstrated superior efficiency in detecting mean changes compared to lower values of λ = 0.01, 0.05, and 0.10. These findings suggest that increasing the smoothing parameter enhances detection power—supporting the current study's use of λ = 0.20 to improve sensitivity in identifying mean changes in the process. For control chart constants, the use of c = 2 in the modified EWMA chart can be shown to perceive mean shifts more rapidly than the original EWMA chart, a result matching the findings of Phanthuna et al. [36]. Additionally, the explicit ARL formula presented in this study significantly reduces computation time while maintaining high accuracy. This result supports the findings presented by Phanthuna et al. [36] and Supharakonsakun et al. [32], confirming the advantage of analytical solutions over iterative numerical methods.

The application of this model to real-world environmental data, such as average monthly rainfall in Bangkok, Thailand, underscores its practical benefits. By effectively identifying shifts in rainfall patterns, the modified EWMA chart can contribute to early warnings in flood and drought risk management, demonstrating its value in environmental monitoring and disaster preparedness.

Overall, evidence from prior studies [19,32,34,36] reinforces that the modified EWMA statistic—characterized by its reduced variance—reliably outpaces long-established control charts in recognizing minor process shifts, both in simulation and real-world applications.

Nevertheless, this study has certain limitations. The model is extended under the notion that the data follow the SARMA$(1,1)_L$ procedure with exponential white noise and known parameters. In practice,

parameter estimation may introduce uncertainty, which could influence the performance of the chart. Additionally, the current formulation of the method may not be directly applicable to other time series models with different seasonal or stochastic characteristics. These limitations offer potential directions for future research, including model generalization, adaptive estimation, and broader testing on diverse real-world datasets.

9 Conclusions

The efficacy of the improved EWMA control chart is clearly confirmed by this research, especially in terms of improving shift detection capabilities for autocorrelated data. The explicit formula derived for the SARMA(1,1)$_L$ process delivers rapid and accurate ARL calculations, making it a preferable method over the traditional NIE approach in terms of computational efficiency. Compared to the standard EWMA chart, the modified version demonstrates enhanced sensitivity and robustness, as evidenced by lower ARL_1 values and a high PCI score. In particular, the PCI value approaches 1, which indicates optimal performance, reinforcing its suitability for environments requiring quick, precise responses and highlighting the chart's superior overall performance in detecting process changes. The successful application of this method to rainfall data in Thailand validates its utility for environmental monitoring. The modified EWMA control chart not only facilitates real-time shift detection but also supports disaster management efforts by enabling proactive risk assessment for extreme weather events. Overall, this research highlights the importance of advanced statistical control methods in improving process monitoring and prediction accuracy, offering significant benefits for both industrial quality control and environmental management applications.

Acknowledgement: The study received monetary support from the National Research Council of Thailand (NRCT), which made the completion of this project possible.

Funding Statement: The research was assisted financially by the National Research Council of Thailand (NRCT) under Contract No. N42A670894.

Author Contributions: The authors contributed to this work as follows: study conception and design: Yadpirun Supharakonsakun; data collection: Yadpirun Supharakonsakun, Yupaporn Areepong; analysis and interpretation of results: Yadpirun Supharakonsakun, Yupaporn Areepong, Korakoch Silpakob; manuscript drafting: Yadpirun Supharakonsakun, Korakoch Silpakob. All authors reviewed the results and approved the final version of the manuscript.

Availability of Data and Materials: The datasets generated and analyzed during the current study are available from the corresponding author on reasonable request.

Ethics Approval: Not applicable.

Conflicts of Interest: The authors declare no conflicts of interest to report regarding the present study.

Appendix A Programming Steps for ARL Calculation

Step 1. Initialize the computation by recording the start time and assigning all required input parameters, including the control chart parameters (λ, c),process parameters (μ, ϕ, θ), and initial values (u, v, z, s).

Step 2. Determine the upper control limit (h) for a fixed lower control limit (g). Compute the numerator of the explicit ARL formula from Eq. (21). Set β_0 =1 for the in-control process (ARL_0), with the target value of 370.

Step 3. Compute the denominator of the explicit ARL formula. For the out-of-control process (ARL_1), set $\beta_1 = \beta_0 (1 + \delta)$ for each shift size. Record the computational time of the explicit formula.

Step 4. Compute the average run length (ARL) using the NIE method based on Eqs. (21)–(23), and record the computational time of the NIE method.

Step 5. Assess the accuracy of the ARL estimates by comparing the explicit formula and the NIE method using the percentage accuracy measure defined in Eq. (24).

Step 6. Evaluate the performance of the control chart using the performance criteria in Eqs. (25) and (26).

Step 7. Summarize the findings and report the results.

References

1. Riaz M, Muhammad F. An application of control charts in manufacturing industry. J Stat Econom Methods. 2012;1(1):77–92.
2. Smajdorova T, Noskievicova D. Analysis and application of selected control charts suitable for smart manufacturing. Processes. Appl Sci. 2012;12(11):5410. doi:10.3390/app12115410.
3. Ottenstreuer S, Weiß CH, Testik MC. A review and comparison of control charts for ordinal samples. J Qual Technol. 2023;55(4):422–41. doi:10.1080/00224065.2023.2170839.
4. Madanhire I, Mbohwa C. Statistical process control (SPC) application in a manufacturing firm to improve cost effectiveness: case study. In: Proceedings of the International Conference on Industrial Engineering and Operations Management (IEOM); 2016 Mar 8–10; Kuala Lumpur, Malaysia. p. 2298–305.
5. Shewhart WA. Economic control of quality of manufactured product. New York, NY, USA: Van Nostrand Company; 1931 [Internet]. [cited 2025 Sep 1]. Available from: https://dspace.gipe.ac.in/xmlui/bitstream/handle/10973/18338/GIPE-009900.pdf.
6. Page ES. Continuous inspection schemes. Biometrika. 1954;41(1/2):100–15. doi:10.1093/biomet/41.1-2.100.
7. Hawkins DM, Olwell DH. Cumulative sum charts and charting for quality improvement. New York, NY, USA: Springer; 1998.
8. Prajapati DR. Effectiveness of conventional CUSUM control chart for correlated observations. Int J Model Optim. 2015;5(2):135–9. doi:10.7763/ijmo.2015.v5.449.
9. Abbas N, Abujiya MR, Riaz M, Mahmood T. Cumulative sum chart modeled under the presence of quilters. Mathematics. 2020;8(2):269. doi:10.3390/math8020269.
10. Roberts SW. Control chart test based on geometric moving average. Technometrics. 1959;1(3):239–50. doi:10.1080/00401706.1959.10489860.
11. Lucas JM, Saccucci MS. Exponentially weighted moving average control schemes: properties and enhancements. Technometrics. 1990;32(1):1–12. doi:10.1080/00401706.1990.10484583.
12. Carson PK, Yeh AB. Exponentially weighted moving average (EWMA) control charts for monitoring an analytical process. Ind Eng Chem Res. 2018;47(2):405–11. doi:10.1021/ie070589b.
13. Petcharat K. Explicit formula of ARL for SMA(Q)L with exponential white noise on EWMA chart. Int J Appl Phys Math. 2016;6(4):218–25. doi:10.17706/ijapm.2016.6.4.218-225.
14. Khan N, Aslam M, Jun C-H. Design of a control chart using a modified EWMA statistic. Qual Reliab Eng Int. 2016;33:1095–104. doi:10.1002/qre.2102.
15. Patel AK, Divecha J. Modified exponentially weighted moving average (EWMA) control chart for an analytical process data. J Chem Eng Mater Sci. 2011;2(1):12–20. doi:10.28991/esj-2023-07-03-014.
16. Zainab MJ, Zoramawa AB, Audu A, Tambuwal AI. Performance of modified exponentially weighted moving average (M-EWMA) control charts using transformed F-distribution. Asian J Probab Stat. 2025;27(3):176–87. doi:10.9734/ajpas/2025/v27i3733.
17. Razailee AS, Ali NM, Kiem KS, Ali N. A comparison between modified EWMA control charts using different robust estimators. Adv Math, Sci J. 2021;10(1):37–44. doi:10.37418/amsj.10.1.5.

18. Hyder M, Raza SMM, Mahmood T, Abbas N. Enhanced dispersion monitoring structures based on modified successive sampling: application to fertilizer production process. Symmetry. 2023;15(5):1108. doi:10.3390/sym15051108.
19. Imtiaz A, Khan N, Saleem M, Aslam M. Development and application of a modified EWMA control chart for early detection of process shifts in skewed distributions. J Chin Inst Eng. 2025;48(1):1–11. doi:10.1080/02533839.2025.2479121.
20. Bodnar R, Bodnar T, Schmid W. Control charts for high-dimensional time series with estimated in-control parameters. Seq Anal. 2024;43(1):103–29. doi:10.1080/07474946.2023.2288135.
21. Aslam A, Khan K, Albassam M, Ahmad L. Moving average control chart under neutrosophic statistics. AIMS Math. 2023;8(3):7083–96. doi:10.3934/math.2023357.
22. Khan I, Noor-ul-Amin M, Khalifa NT, Ashad A. EWMA control chart using Bayesian approach under paired ranked set sampling schemes: an application to reliability engineering. AIMS Math. 2023;8(9):20324–50. doi:10.3934/math.20231036.
23. Crowder SV. A simple method for studying run length distributions of exponentially weighted moving average charts. Technometrics. 1987;29(4):401–7. doi:10.1080/00401706.1987.10488267.
24. Champ CW, Rigdon SE. A comparison of the Markov chain and the integral equation approaches for evaluating the run length distribution of quality control charts. Commun Stat Simul Comput. 1991;20(1):191–204. doi:10.1080/03610919108812948.
25. Harris TJ, Ross WH. Statistical process control procedures for correlated observations. Can J Chem Eng. 1991;69(1):48–57. doi:10.1002/cjce.5450690106.
26. VanBrackle L, Reynolds MR. EWMA and CUSUM control charts in the presence of correlation. Commun Stat Simul Comput. 1997;26:979–1008. doi:10.1080/03610919708813421.
27. Paichit P, Areepong Y, Sukparungsee S. Average run length of EWMA chart for SARMA (P, Q)$_L$ processes. Int J Appl Math Stat. 2014;80(1):85–103.
28. Polyeam D, Phanyaem S. Application of EWMA control chart for analyzing changes in SAR(P)L model with quadratic trend. Math Stat. 2025;13(3):163–74.
29. Khan N, Aslam M, Albassam M. Efficiency enhancement of the modified EWMA control method with conditional expected delay for change detection in processes. Front Appl Math Stat. 2023;9:1268340. doi:10.3389/fams.2023.1268340.
30. Alevizakos V, Chatterjee K, Koukouvinos C. Modified EWMA and DEWMA control charts for process monitoring. Commun Stat Theory Methods. 2022;51(21):7390–412. doi:10.1080/03610926.2021.1872642.
31. Haq A, Woodall WH. A critique of the use of modified and moving average-based EWMA control charts. Qual Reliab Eng Int. 2023;39(4):1269–76. doi:10.1002/qre.3290.
32. Supharakonsakun Y, Areepong Y, Sukparungsee S. Monitoring the process mean of a modified EWMA chart for ARMA(1,1) process and its application. Suranaree J Sci Technol. 2020;27(4):1–11. doi:10.7717/peerj.10467.
33. Saghir A, Ahmad L, Aslam M. Modified EWMA control chart for transformed gamma data. Commu Stat Simul Comput. 2021;50(10):3046–59. doi:10.1080/03610918.2019.1619762.
34. Paichit P, Peerajit W. The average run length for continuous distribution process mean shift detection on a modified EWMA control chart. Asia-Pac J Sci Technol. 2022;27:109–18.
35. Niaz A, Khan M, Ijaz M. One-sided modified EWMA control charts for monitoring time between events. Qual Reliab Eng Int. 2025;41(4):1293–318. doi:10.1002/qre.3718.
36. Phanthuna P, Areepong Y, Sukparungsee S. Exact run length evaluation on a two-sided modified exponentially weighted moving average chart for monitoring process mean. Comput Model Eng Sci. 2021;127(1):23–41. doi:10.32604/cmes.2021.013810.
37. Richard SP. A simple proof of the Banach contraction principle. J Fixed Point Theory Appl. 2007;2(2):221–3. doi:10.1007/s11784-007-0041-6.
38. Phanthuna P, Areepong Y, Sukparungsee S. Numerical integral equation methods of average run length on modified EWMA control chart for exponential AR(1) process. In: Proceedings of the International MultiConference of Engineers and Computer Scientists (IMECS); 2018 Mar 14–16; Hong Kong, China. p. 845–7.

39. Areepong Y. An integral equation approach for analysis of control charts [dissertation]. Sydney, Australia: University of Technology Sydney; 2009.
40. Alevizakos V, Chatterjee K, Koukouvinos C. The trip exponentially weighted moving average control chart. Qual Technol Quant Manag. 2021;18(3):326–54. doi:10.1080/16843703.2020.1809063.
41. Monthly rainfall data for all areas of Thailand [Internet]. Bangkok, Thailand: Hydro-Informatics Institute (HII). [cited 2024 Nov 14]. Available from: https://data.hii.or.th/dataset/spatial-rain/resource/be424ef5-be5b-4f62-b147-6a569179e22b.